

Electromagnetic form factors of the $A = 3$ systems

E. Hadjimichael

Department of Physics, Fairfield University, Fairfield, Connecticut 06430

B. Goulard and R. Bornais

Laboratory of Nuclear Physics, University of Montreal, Montreal, Quebec, Canada H3C 3J7

(Received 26 August 1982)

We explore the dependence of the magnetic and charge form factors of ${}^3\text{He}$ and ${}^3\text{H}$ on nucleon structure models and NN interaction models within the traditional framework of nucleons, isobars, and mesons. We utilize wave functions which incorporate the effect of a genuine three-body force, and include contributions to the nuclear current from a variety of mesonic exchange and isobaric processes. The importance of the high momentum transfer region as a source of information on short-range processes in the nuclear medium is reiterated by our results.

NUCLEAR STRUCTURE Trinucleon systems; electromagnetic form factors; three-body force and mesonic exchange currents.

I. INTRODUCTION

Our present understanding of nuclear phenomena is in a state of "creative discontent." The basically nonrelativistic dynamical theories involving point-like nucleons, isobars, and mesons lead to theoretical predictions which appear to be in disagreement with globally available nuclear data by as much as 10% to 15%. It is not clear how much, if any, of this discrepancy could be cured by relativistic considerations. Difficulties associated with the introduction of relativistic aspects into nuclear dynamics have so far discouraged widespread efforts in this direction. At the same time the emergence of the view that quantum chromodynamics (QCD) may be the fundamental theory of strong interactions is promoting the perception that a search for more basic microscopic processes than meson exchanges, derived from QCD principles, is in order now. This search is still in a very preliminary stage, but the possibility that a more complete solution to the "nuclear problem" may emerge through a QCD-based theory with quarks and gluons as the fundamental units of strongly interacting matter is attracting a great deal of attention. Our interest is not focused merely on phenomena where individual quarks respond incoherently to an external probe, e.g., at high values of momentum transfer, but also on phenomena where the quarks in a hadron may respond collectively and coherently to an external probe; it remains to be seen whether or not under these latter circumstances a composite hadron can still be treated

as an "elementary" particle as in the hitherto traditional theories. This point, in fact, is of central importance in current nuclear investigations.

Outstanding among the nuclear observables that could help provide guidance regarding the role of hadron quark-compositeness in the nuclear bound system are the four elastic electron-scattering form factors (charge and magnetic) of the $A=3$ systems, ${}^3\text{He}$ and ${}^3\text{H}$. Our experience so far, based on theoretical investigations within the traditional theory of the nuclear interaction phenomenon, indicates that these form factors as functions of momentum transfer q are capable of posing constraints on the content of theoretical models, provided that we survey an extensive range of momentum transfer q . Extrapolating from this state of affairs, we may optimistically predict that if there is truly a need to augment the present theories by including quark-based dynamical processes then this need will become apparent as we probe more rigorously the electromagnetic form factors of ${}^3\text{He}$ and ${}^3\text{H}$.

We recall that the cross section for elastic electron-nucleus scattering is

$$d\sigma/d\Omega = (\epsilon'/\epsilon)\sigma_M [A(q_\mu^2) + B(q_\mu^2)\tan^2(\theta/2)], \quad (1)$$

where θ is the electron scattering angle, ϵ' and ϵ are the final and initial electron energies, and σ_M is the Mott cross section. The spin = $\frac{1}{2}$ character of ${}^3\text{He}$ and ${}^3\text{H}$ dictates that the structure functions A and B have the form

$$A(q_\mu^2) = \frac{F_C^2(q_\mu^2) + \tau F_M^2(q_\mu^2)}{1 + \tau}, \quad (2)$$

$$B(q_\mu^2) = 2\tau F_M^2(q_\mu^2),$$

where $\tau = q_\mu^2 / 4M_T^2$ and F_C and F_M are the charge and magnetic form factors. M_T is the nuclear mass. The experimental data for $F_C(q^2)$ and $F_M(q^2)$ of ${}^3\text{He}$ extend to $q \sim 9 \text{ fm}^{-1}$ and $q \sim 5.5 \text{ fm}^{-1}$, respectively, while those for ${}^3\text{H}$ are limited presently to the low q region ($\leq 3.0 \text{ fm}^{-1}$). Fortunately, measurements of $e\text{-}{}^3\text{H}$ scattering are now in their initial stage at both the Bates-M.I.T. and the Saclay electron facilities.¹ The simultaneous investigation of ${}^3\text{He}$ and ${}^3\text{H}$ will reduce somewhat the impact of theoretical uncertainties and will allow for a more precisely directed exploration of nuclear dynamics.

In the last decade or so there have been several efforts to calculate the charge form factor of ${}^3\text{He}$,²⁻⁸ while only moderate effort has been invested in the magnetic form factor of this nucleus.^{9,10} Because of the scarcity of data ${}^3\text{H}$ has not attracted as much attention so far, but this is bound to change presently. Due to long-standing discrepancies in the region $q < 5.0 \text{ fm}^{-1}$, the charge form factor of ${}^3\text{He}$ became the subject of wide-ranging discussions. The early calculations for F_C and F_M , treating the trinucleon as an S -state system and the electromagnetic interaction in the impulse approximation, were gradually augmented by the introduction of the nuclear D state,^{2,3,7} isobaric admixtures in the nuclear wave function,^{2,5,6} and mesonic-exchange currents (MEC) arising from a small number of meson-exchange processes^{2,4} and later from a more complete set of mesonic processes⁸ and isobaric processes^{5,8}; in addition, the role of the three-body force has been explored in the case of F_C .⁸ In a recent paper we reported that we can successfully predict the magnitude of the charge form factor of ${}^3\text{He}$ at the position of the second maximum by taking into account MEC effects, isobaric currents, the contribution from at least a portion of the three-body force, and the small relativistic-order contributions to the single body charge density. Beyond $q \approx 6.0 \text{ fm}^{-1}$, however, there remain discrepancies which afford ample opportunity for testing further improvements to traditional models, as well as QCD-inspired ideas and nontraditional quark-based models.

In this paper, we endeavor to explore the dependence of the form factors of ${}^3\text{He}$ and ${}^3\text{H}$ on a variety of theoretical inputs, all within the traditional framework of nucleons, isobars, and mesons. We pay particular attention to nucleon electromagnetic structure, the NN force, and the meson-nucleon vertex functions as well as the three-body force and mesonic and isobaric currents. This is the first time

when all these elements are brought together in a single calculation of the magnetic form factors; hence there is an enhanced completeness in the theoretical predictions reported here which, it is hoped, will help delineate clearly the course of future investigations in this area. In the same vein, the investigation of theoretical input in the case of the charge form factors is equally instructive.

This paper is organized as follows. In Sec. II we describe the theoretical ingredients of the present calculation and present our most complete theoretical predictions in comparison with available data. One of our major concerns, however, is the degree to which the trinucleon form factors are sensitive to models of the nucleon structure, meson-nucleon vertices, the NN force, and the three-body force. Hence we devote Sec. III to this topic. We present extensive results in graphical form hoping to illustrate the model dependence and hence the physics underlying the structure of $A=3$ nuclei. Finally, in Sec. IV we discuss our theoretical predictions and make deductions based on them.

II. THEORETICAL INGREDIENTS AND RESULTS

The physical processes that we have considered to contribute to $e\text{-}{}^3\text{He}$ and $e\text{-}{}^3\text{H}$ scattering are shown in Fig. 1. They include the impulse approximation (IA) without and with isobaric admixture in the nuclear wave function, Figs. 1(a) and (b), respectively, isobaric excitations involving two and one nucleon, Figs. 1(c) and (d) and Fig. 1(e), respectively, and two-body mesonic processes (MEC), Figs. 1(f)–(k). Note that a ρ -exchange seagull term (ρ_{s1}) is also included in addition to the $\rho N\bar{N}$ process. The procedure for deriving the nuclear current $J=(\vec{J},\rho)$ which interacts with the external electromagnetic field A is to start with the covariant amplitude for the processes in Fig. 1 (Ref. 11) and, following a

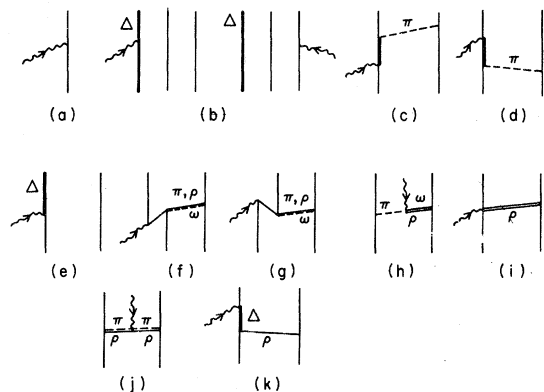


FIG. 1. Mesonic and isobaric processes that have been taken into account in this work.

nonrelativistic reduction, the photon-nucleus interaction Hamiltonian H is derived and cast in the form

$$H = J_\mu A_\mu,$$

thus identifying the nuclear current $J = J^{(1)} + J^{(2)}$, where $J^{(1)}$ is the single-body (IA) current and $J^{(2)}$ is the contribution from MEC. We treat the nucleons in the static limit and hence we keep only lower-order terms in $(1/M)$, where M is the nucleon mass.

The results for $\vec{J}^{(2)}$ derived in this manner are in agreement with those derived by the application of powerful low-energy theorems.¹¹ $J^{(1)}$, $J^{(2)}$, and the NN potential V_{NN} derived from boson-exchange processes [as in Figs. 1(f), (g), (i), and (j) in the absence of the photon line] are of the same order in $(1/M)$. Unfortunately, there are no low-energy theorems that yield results for $\rho^{(2)}$. This quantity is of higher order in $(1/M)$ and hence is of a relativistic order of magnitude. The fact that the usual boson-exchange NN potentials that are utilized to derive the nuclear wave functions have no relativistic-order effects makes for a certain inconsistency in the evaluation of the matrix elements of $\rho^{(2)}$. A portion of the contribution from the NN interaction phenomenon to the charge distribution is missing and hence our evaluation of the charge form factors is less complete than that of the magnetic form factors. It is not within the scope of the present work to remedy this situation—one would need to introduce relativistic dynamics into the NN theory. Nevertheless, there is redeeming value in this work in that it demonstrates the capacity of the conventional theory, including MEC, to predict the charge distribution in the three-body system.

The trinucleon wave functions utilized in these calculations have been derived by the Grenoble group¹² by solving the Faddeev equations in coordinate space. We are interested in assessing the sensitivity of the form factors to such NN interaction characteristics as the short range part, the tensor part, the asymptotic normalization, etc., and, by extension, in testing the underlying processes that give rise to these characteristics. For this purpose we utilize the solutions derived from four different NN potentials, namely, the Malfliet-Tjon (MT) model¹³ which has no tensor part, the Paris model,¹⁴ the Sprung-de Turreil (SdT) and Sprung-Rouben-de Turreil (SRdT) models,¹⁵ and the Reid soft core (R) (Ref. 16) model. In addition, we have attempted to answer the question regarding the role of a possible three-body force. Hence a genuine three-body force derived from the process shown in Fig. 2(a) is utilized,¹² in conjunction with the SdT NN interaction, in the Faddeev formalism and the resulting wave functions are used to calculate the matrix elements

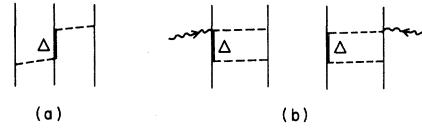


FIG. 2. (a) Microscopic process giving rise to a three-nucleon force. (b) Two-pion exchange processes with isobars that may contribute to the three-body form factors, Ref. 31.

of J . It should be noted that this three-body force leads to an increase of the ${}^3\text{H}$ binding energy by 650 keV.

Another point of interest is the physical size of the nucleon in the nuclear medium. In traditional NN theories the nucleon size effects are not derived from first principles but are incorporated into the exchange theories by hadronic form factors appended to meson-nucleon vertices of the general form

$$F_{VNN}(q^2) = \frac{\Lambda_V^2 - \mu_V^2}{\Lambda_V^2 + Q^2}, \quad (3)$$

where μ_V is the mass of the exchanged meson and Q is its momentum. Λ_V is a constant determined phenomenologically. For π exchange, for example, Λ_π is of the order of ~ 1.2 GeV, determined from fits to πN scattering data. This translates to a πN interaction volume with a radius $r \sim 0.33$ fm, reflecting a small, almost pointlike nucleon. In contrast, experimental data for electron-nucleon scattering suggests a charge radius for the proton of about 0.8 fm. The MEC effects are naturally dependent upon the size of the nucleons in the nuclear medium. We explore this dependence by allowing Λ_π to acquire values < 1.2 GeV, thus effectively simulating large-size nucleons.

In addition, there are several models presently in use of the electromagnetic form factors of nucleons. While most of them tend to agree for low q values, they begin to diverge in their predictions for $q \sim 5.0$ fm^{-1} . In particular, the electric form factor of the neutron has been difficult to determine so far and may remain an uncertain variable until perhaps polarization transfer experiments and (e, n) coincidence experiments¹⁷ can be performed in a future, high energy, high duty factor electron facility. In the present work we explore the dependence on nucleon electromagnetic form factors by employing four different models [Janssens *et al.*¹⁸ (J), monopole (M) and dipole (D) forms of the Iachello-Jackson-Lande (IJL) model,¹⁹ and the Blatnik-Zovko (B)²⁰]; we compare these with results obtained for point nucleons.

Our final results for the charge form factors F_C of ${}^3\text{He}$ and ${}^3\text{H}$ are shown in Figs. 3(a) and (b) and

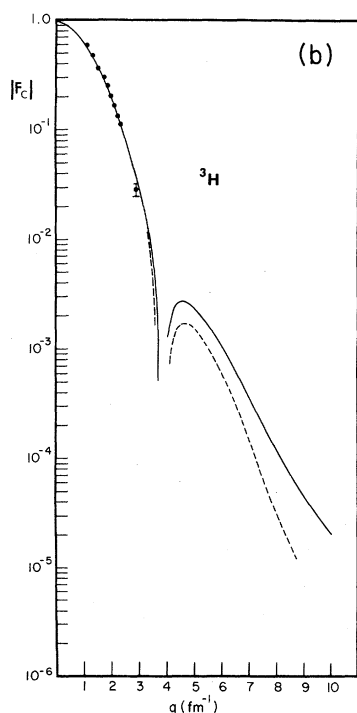
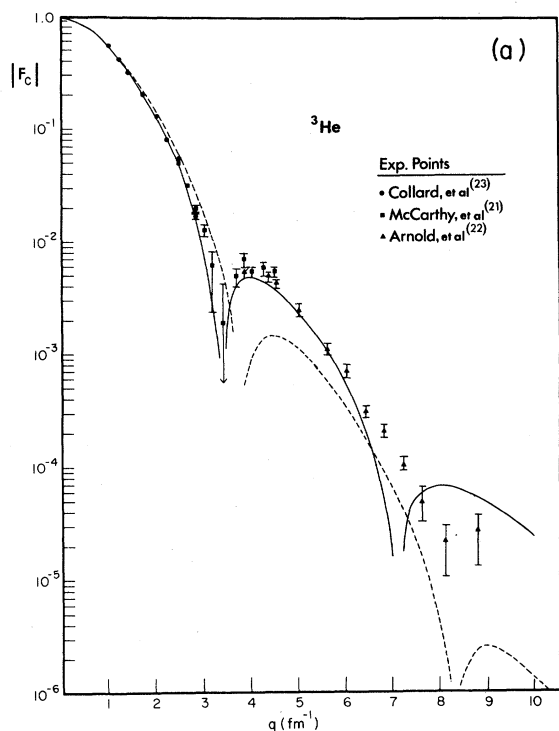


FIG. 3. (a) The IA (dashed line) and full result (solid line) of the charge form factor of ${}^3\text{He}$. The effects of the three-body force are included in these results. (b) The charge form factor of ${}^3\text{H}$; see text for details. Experimental points are from Refs. 21–23.

Table I. The three-body wave functions were calculated with the SdT NN interaction and incorporate the effects of the three-body force as explained earlier. We have utilized the Blatnik-Zovko model for the nucleon electromagnetic form factors and have set the parameter Λ_π in the vertex functions of the dominant pion-exchange processes equal to 6.0 fm^{-1} . For the ρ - and ω -exchange processes, $\Lambda_V = 7.31 \text{ fm}^{-1}$ was used. Our results for the magnetic form factors of ${}^3\text{He}$ and ${}^3\text{H}$, evaluated with the same input, are shown in Figs. 4(a) and (b) and Table II. It should be mentioned that the IA results for F_M contain the contribution from the nucleon convection current, and the IA results for F_C incorporate the Foldy-Darwin and spin-orbit contributions to the single-body charge density. The MEC and isobaric processes that were included in this calculation are those from Fig. 1.

The data points in Figs. 3 and 4 are taken from Refs. 21–26. The results shown in these figures verify the fact that, within the traditional theory of nuclear physics, MEC effects are indispensable for predicting with some success, albeit limited, the experimental data.

A. Charge form factors

Our results at $q \sim 0.3 \text{ fm}^{-1}$ yield a charge rms radius equal to 1.92 fm for ${}^3\text{He}$ and 1.71 fm for ${}^3\text{H}$. These are in good agreement with the experimental values of 1.88 and 1.70 fm , respectively.

The theoretical predictions for the charge form factor of ${}^3\text{He}$ are also satisfactory for values of momentum transfer in the region $q < 6.0 \text{ fm}^{-1}$. The first diffraction minimum is accurately localized and, importantly, the long-standing discrepancy in the region of the second maximum is finally resolved.

However, the theoretical results fall below the data points in the region $6.0 \text{ fm}^{-1} \leq q \leq 7.0 \text{ fm}^{-1}$. It is also significant that these results display a second diffraction minimum at $q \sim 7.0 \text{ fm}^{-1}$ and a third maximum at $q \sim 8.5 \text{ fm}^{-1}$. This characteristic structure is present independently of the nucleon electromagnetic structure models and NN interaction models used in the calculation (see Sec. III). In this high- q region it is also thought to be likely that nucleon-meson dynamics may have to be abandoned in favor of quark-gluon dynamics. If this is so, it is important to note the fact that dimensional scaling quark models²⁷ and relativistic harmonic oscillator quark models of ${}^3\text{He}$ (Ref. 28) yield a structureless behavior for F_C in the high- q region in contrast to the theoretical results in Fig. 3(a). The data presently available are too sparse and uncertain to favor either the nucleon-meson theory or the quark-gluon theory at $q > 6.0 \text{ fm}^{-1}$, but it is obvious that it is

TABLE I. Charge form factor F_C of ${}^3\text{He}$ and ${}^3\text{H}$. These results have been calculated with the SdT NN interaction, the three-body force, and the Blatnik-Zovko model for nucleon form factors. They correspond to Fig. 3.

q (fm^{-1})	${}^3\text{He}$		${}^3\text{H}$	
	IA	Total	IA	Total
0.0	1.0	1.0	1.0	1.0
0.5	0.865	0.849	0.868	0.868
1.0	0.571	0.556	0.604	0.604
1.5	0.308	0.294	0.347	0.347
2.0	0.141	0.129	0.170	0.169
2.5	0.552×10^{-1}	0.445×10^{-1}	0.719×10^{-1}	0.705×10^{-1}
3.0	0.174×10^{-1}	0.890×10^{-2}	0.252×10^{-1}	0.236×10^{-1}
3.5	0.322×10^{-2}	-0.276×10^{-2}	0.612×10^{-2}	0.462×10^{-2}
4.0	-0.919×10^{-3}	-0.480×10^{-2}	-0.294×10^{-3}	-0.162×10^{-2}
4.5	-0.150×10^{-2}	-0.376×10^{-2}	-0.171×10^{-2}	-0.279×10^{-2}
5.0	-0.112×10^{-2}	-0.232×10^{-2}	-0.152×10^{-2}	-0.235×10^{-2}
5.5	-0.673×10^{-3}	-0.123×10^{-2}	-0.102×10^{-2}	-0.163×10^{-2}
6.0	-0.349×10^{-3}	-0.549×10^{-3}	-0.595×10^{-3}	-0.102×10^{-2}
6.5	-0.162×10^{-3}	-0.185×10^{-3}	-0.316×10^{-3}	-0.611×10^{-3}
7.0	-0.659×10^{-4}	-0.124×10^{-4}	-0.154×10^{-3}	-0.355×10^{-3}
7.5	-0.223×10^{-4}	0.532×10^{-4}	-0.696×10^{-4}	-0.206×10^{-3}
8.0	-0.445×10^{-5}	0.679×10^{-4}	-0.285×10^{-4}	-0.121×10^{-3}
8.5	0.133×10^{-5}	0.608×10^{-4}	-0.101×10^{-4}	-0.735×10^{-4}
9.0	0.251×10^{-5}	0.475×10^{-4}	-0.261×10^{-5}	-0.462×10^{-4}
9.5	0.203×10^{-5}	0.344×10^{-4}	-0.691×10^{-6}	-0.303×10^{-4}

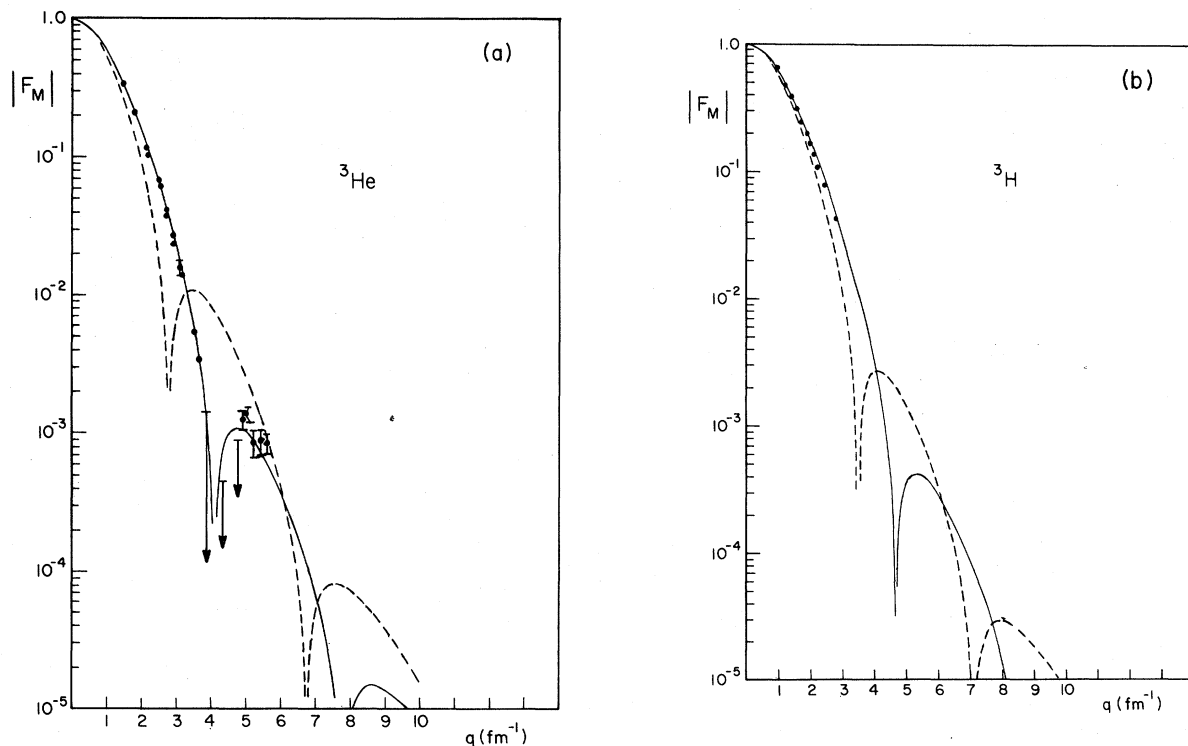


FIG. 4. (a) The IA (dashed line) and full result (solid line) of the magnetic form factor of ${}^3\text{He}$; these results include the effects of the three-body force. (b) The magnetic form factor of ${}^3\text{H}$; see text for details. Experimental points are from Refs. 23–26.

TABLE II. Magnetic form factor F_M of ${}^3\text{He}$ and ${}^3\text{H}$. These results have been calculated with the SdT NV interaction, the three-body force, and the Blatnik-Zovko model for nucleon form factors. They correspond to Fig. 4. Theoretical magnetic moments used to normalize the form factors:

$$\mu^{\text{IA}}({}^3\text{He}) = -1.76 \mu_N, \quad \mu^{\text{total}}({}^3\text{He}) = -2.18 \mu_N,$$

$$\mu^{\text{IA}}({}^3\text{H}) = 2.57 \mu_N, \quad \mu^{\text{total}}({}^3\text{H}) = 3.01 \mu_N.$$

q (fm^{-1})	${}^3\text{He}$		${}^3\text{H}$	
	IA	Total	IA	Total
0.0	1.0	1.0	1.0	1.0
0.5	0.843	0.863	0.861	0.874
1.0	0.522	0.576	0.566	0.599
1.5	0.246	0.317	0.298	0.345
2.0	0.873×10^{-1}	0.151	0.130	0.172
2.5	0.163×10^{-1}	0.625×10^{-1}	0.462×10^{-1}	0.770×10^{-1}
3.0	-0.719×10^{-2}	0.221×10^{-1}	0.113×10^{-1}	0.307×10^{-1}
3.5	-0.107×10^{-1}	0.587×10^{-2}	-0.313×10^{-3}	0.108×10^{-1}
4.0	-0.818×10^{-2}	0.358×10^{-3}	-0.274×10^{-2}	0.301×10^{-2}
4.5	-0.494×10^{-2}	-0.990×10^{-3}	-0.232×10^{-2}	0.349×10^{-3}
5.0	-0.257×10^{-2}	-0.975×10^{-3}	-0.143×10^{-2}	-0.343×10^{-3}
5.5	-0.116×10^{-2}	-0.665×10^{-3}	-0.740×10^{-3}	-0.401×10^{-3}
6.0	-0.419×10^{-3}	-0.376×10^{-3}	-0.321×10^{-3}	-0.287×10^{-3}
6.5	-0.826×10^{-4}	-0.183×10^{-3}	-0.107×10^{-3}	-0.171×10^{-3}
7.0	0.480×10^{-4}	-0.711×10^{-4}	-0.104×10^{-4}	-0.882×10^{-4}
7.5	0.798×10^{-4}	-0.153×10^{-4}	0.233×10^{-4}	-0.390×10^{-4}
8.0	0.735×10^{-4}	0.840×10^{-5}	0.296×10^{-4}	-0.132×10^{-4}
8.5	0.554×10^{-4}	0.148×10^{-4}	0.253×10^{-4}	-0.160×10^{-5}
9.0	0.379×10^{-4}	0.138×10^{-4}	0.188×10^{-4}	0.247×10^{-5}
9.5	0.241×10^{-4}	0.978×10^{-5}	0.125×10^{-4}	0.276×10^{-5}

this high q region dominated by short-range processes that offers the best test for contesting theoretical ideas regarding the nuclear medium. In the case of ${}^3\text{H}$, an excellent agreement between the available low q data and our theoretical results is noted in Fig. 3(b).

We next examine the charge density $\rho_C(r)$. Figure 5 displays $\rho_C(r)$ of ${}^3\text{He}$, obtained by Fourier-transforming the charge form factor, e.g.,

$$\rho_C(r) = \frac{Z}{2\pi^2} \int dq q^2 \left(\frac{\sin qr}{qr} \right) F_C(q^2). \quad (4)$$

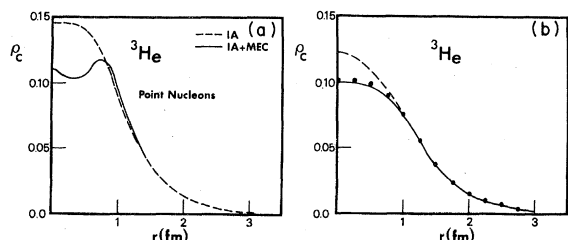


FIG. 5. (a) The charge density distribution $\rho_C(r)$ of ${}^3\text{He}$ for point nucleons; the dashed line is the IA result. (b) $\rho_C(r)$ of ${}^3\text{He}$ for physical nucleons described by the Blatnik-Zovko model. The dashed line is the IA result.

Figure 5(a) shows the charge density for point nucleons and 5(b) shows the physical charge density corresponding to the charge form factor in Fig. 3(a), along with quasiexperimental data points. The IA result is also shown (dashed line). In Fig. 5(a) one notes that the central depression in the full (IA + MEC) result reverses itself and develops a small rise very close to the center of the nucleus. This is easily understood by observing that the charge density at $r=0$ becomes

$$\rho_C(r=0) = \frac{Z}{2\pi^2} \int dq q^2 F_C(q^2)$$

so that F_C at high q values is heavily weighed due to the q^2 factor in the integrand. This, in conjunction with the fact that F_C for point nucleons has a very prominent (positive) third maximum at $q \sim 8.0 \text{ fm}^{-1}$ (see Fig. 12), is finally responsible for the rise in $\rho_C(r)$.

The physical charge density for ${}^3\text{H}$ is shown in Fig. 6. The IA result is given by the dashed line. In both ${}^3\text{He}$ and ${}^3\text{H}$ the effect of the MEC processes is to reduce the charge distribution near the nuclear center. Mathematically, this reduction in the value of $\rho_C(r)$ is accomplished by the narrowing of the re-

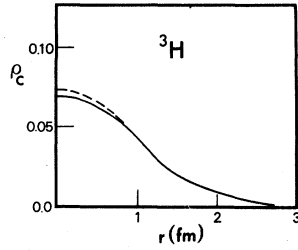


FIG. 6. The charge density distribution $\rho_C(r)$ of ${}^3\text{H}$ for physical nucleons described by the Blatnik-Zovko model. The dashed line is the IA result.

gion where F_C is dominantly positive ($q < 3.5 \text{ fm}^{-1}$) and/or the buildup of F_C in the region where it is negative ($q > 3.5 \text{ fm}^{-1}$). This is an illustration of the intimate relation between form factor and density characteristics.

In an earlier publication²⁹ we addressed the question of the extraction of a quasiexperimental single-body charge distribution for point nucleons, which has attracted some attention in recent years.³⁰ We showed that there is no unambiguous way to determine this quantity, and, in particular, its form near the origin is totally beyond our reach at this point.²⁹ Hence we have no unambiguous (quasi)experimental results to compare with the theoretical estimates shown in Fig. 5(a).

B. Magnetic form factors

The magnetic form factor F_M is displayed and compared with experimental results in Figs. 4(a) and (b) for ${}^3\text{He}$ and ${}^3\text{H}$, respectively. Our estimates for the magnetic moments are

$$\mu({}^3\text{He}) = -2.188$$

and

$$\mu({}^3\text{H}) = 3.016$$

in units of μ_N ($\mu_N =$ nuclear magneton) (the corresponding IA results are -1.760 and $2.568 \mu_N$, respectively). The experimental magnetic moments are known very accurately to be

$$\mu_{\text{exp}}({}^3\text{He}) = -2.128$$

and

$$\mu_{\text{exp}}({}^3\text{H}) = 2.979,$$

in units of μ_N . Hence our theoretical results overestimate the data by only 2.8% and 1.2%, respectively, at $q=0.0 \text{ fm}^{-1}$.

The most recent measurements of the magnetic form factor of ${}^3\text{He}$ at Bates-M.I.T. and at Saclay ex-

tend our knowledge of this quantity to $q \sim 5.5 \text{ fm}^{-1}$. The results clearly identify a first diffraction minimum in the neighborhood of 4.0 fm^{-1} and a second maximum at about $q \sim 5.0 \text{ fm}^{-1}$. These features are correctly localized by our theoretical results which incorporate the effect from the three-body force, as seen in Fig. 4(a). The latter lowers the contribution from the nuclear current employed in our calculation, in the region of the second maximum. Indeed, the magnitude of F_M at the second maximum appears underestimated; this deficiency is independent of nucleon electromagnetic structure models and NN interaction models (see Sec. III). The most likely source for this discrepancy is lack of completeness in the nuclear current. Continued investigations in this area may still uncover mesonic exchange processes additional to those in Fig. 1, which could help improve the agreement with data in this middle region of q . Alternatively, quark processes in the domain where perturbative QCD is valid may furnish the proper enhancement of the nuclear current.

As with the charge form factor, the high q region of the magnetic form factor will prove particularly useful in testing theoretical ideas on short-range processes in the nuclear medium. So far, the data for ${}^3\text{H}$ are very limited and those for ${}^3\text{He}$ have just begun to probe the interesting momentum region. Our theoretical results show structure characteristics at high q , for both ${}^3\text{He}$ and ${}^3\text{H}$, that are qualitatively peculiar to mesonic exchange theories and quantitatively sensitive to nucleon structure and NN interaction models (see Sec. III).

It is also interesting to examine the distribution of magnetization in the three-body systems. Hence, we derive the magnetization density $\rho_M(r)$ by Fourier transforming the magnetic form factor [e.g., by Eq. (4) where $ZF_C(q^2)$ is replaced by $\mu F_M(q^2)$, μ equals nuclear magnetic moment]. The results for ${}^3\text{He}$ are shown in Fig. 7(a) for point nucleons and in Fig. 7(b) for nucleons described by the Blatnik-Zovko model.²⁰ The IA results are shown again by dashed lines. In the case of $\rho_M(r)$, we note that the effect of MEC processes is to enhance substantially the magnetization density of ${}^3\text{He}$ within 1 fm from the nuclear center, e.g., the MEC contributions have the opposite effect here than in the case of the charge density. Mathematically this comes about by the enlargement of the momentum region where F_M is dominantly negative [from $q \sim 2.7$ to 4.0 fm^{-1} in (IA + MEC) results]. The central depression in the IA result for point nucleons is due to the rather prominent second diffraction maximum (positive) from 3.0 fm^{-1} to about 7.0 fm^{-1} .

The ${}^3\text{He}$ data for $F_M(q^2)$ are not sufficiently extensive to allow us to obtain reliably from them an

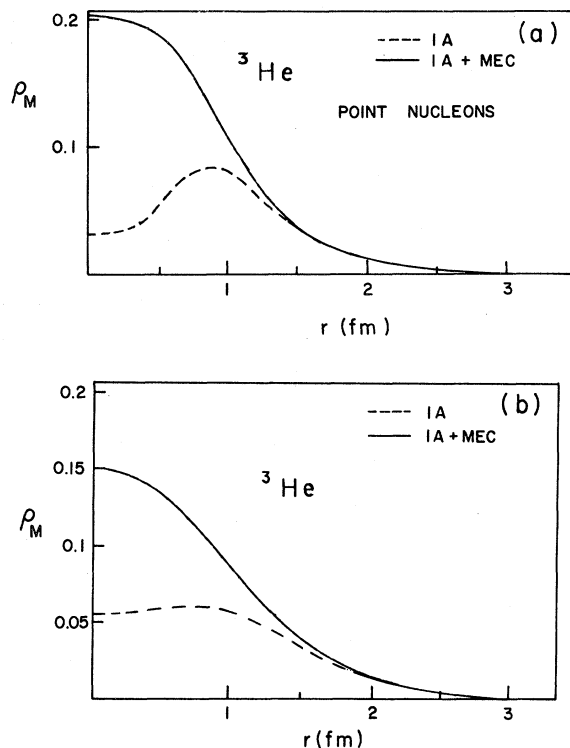


FIG. 7. (a) The magnetization density $\rho_M(r)$ of ${}^3\text{He}$ for point nucleons. (b) $\rho_M(r)$ of ${}^3\text{He}$ for physical nucleons described by the Blatnik-Zovko model. The dashed line is the IA result.

experimental magnetization density which we could compare to our theoretical predictions. Hence, this situation is less informative than the corresponding one for F_C . However, to the extent that the high- q behavior of F_M is determined by two-body effects, as indeed the case appears to be, it is the short-range two-body microscopic processes that are instrumental in defining the nuclear magnetization density in the nuclear interior. These are obviously the same processes that are responsible for the medium and short-range NN dynamics and, by necessity, they are intimately related to nucleonic structure. It is therefore appropriate at this point to look into the dependence of F_C and F_M on NN interaction models and nucleon structure models.

III. SENSITIVITY OF THE FORM FACTORS TO THEORETICAL INPUT

In spite of a great deal of theoretical work on NN dynamics in the last 20 years or so, our understanding of the medium range and, in particular, the short-range microscopic processes contributing to the interaction phenomenon is not on a firm basis. Even within the traditional framework of nucleons,

isobars, and mesons, different models of the NN interaction currently in vogue incorporate different medium and short-range microscopic processes and encounter difficulties in reproducing data over an extensive energy range. Intimately related to NN dynamics is the question of nucleon structure characteristics, such as the nucleon size.

The differences among different NN and nucleon theoretical models do not become apparent at low values of q in electron scattering estimates. In the medium and, in particular, in the high- q region, however, the differences are rather striking, as expected. In this section we would like to explore the sensitivity of the electromagnetic form factors of ${}^3\text{He}$ and ${}^3\text{H}$ to different theoretical inputs and thus identify areas where further work might be useful in promoting our understanding of the interaction phenomena.

Here the discussion is limited to ${}^3\text{He}$; equivalent deductions can be made on the basis of the ${}^3\text{H}$ results. We begin by showing the individual MEC contributions to the charge form factor in Fig. 8, and to the magnetic form factor in Fig. 9. As has been documented before (Refs. 2–4,8,9), the contribution from the pion “pair” process (πNN) dominates in both cases. In Fig. 8 we display also a non-MEC result denoted as R ; this is the combined contribution of the (relativistic order) Darwin-Foldy and spin-orbit terms in the single-body charge operator. This contribution is essentially of the same order of magnitude as the dominant πNN term and hence it is not appropriate to disregard it as has been the practice in the past. The results in Figs. 8 and 9 have been evaluated with three-body wave functions found with the SdT potential and incorporate the three-body force. The Blatnik-Zovko model and $\Lambda_\pi = 6.0 \text{ fm}^{-1}$ have been utilized here.

Figures 10 and 11 show explicitly the effect of the three-body force on the IA results [$\Delta(\text{IA})_{3b}$], and on the MEC results [$\Delta(\text{MEC})_{3b}$], in the case of F_C and F_M , respectively. $(\text{IA})_{2b}$ and $(\text{MEC})_{2b}$ are the IA and MEC contributions without the benefit of the three-body force. We note that in the low and medium q region the three-body force corrections are a factor of 10 to 100 smaller than the main terms. In the high- q region, however ($> 7.0 \text{ fm}^{-1}$), the corrections are a large fraction of the main terms.

It is worth mentioning that the D -state admixture in the three-body system increases from 7.9% to 8.5% when the three-body force is taken into account. This is reflected primarily in MEC contributions at high q values.

The dependence of the form factors on nucleon electromagnetic structure models is shown in Figs. 12 and 13 for ${}^3\text{He}$ and ${}^3\text{H}$, respectively. The Janssens *et al.* model J is based on best fits of exper-

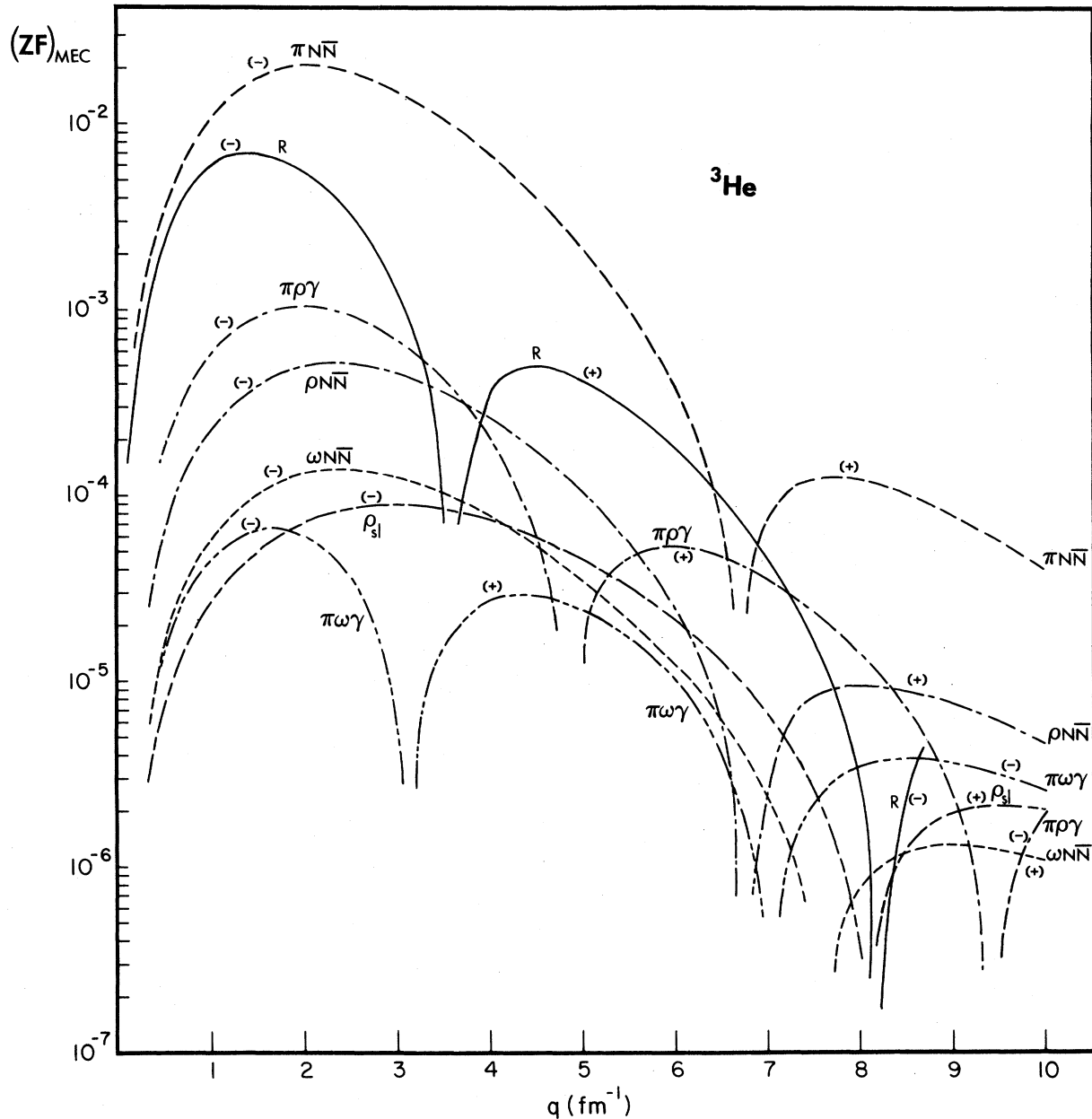


FIG. 8. MEC contributions to the charge form factor of ${}^3\text{He}$, corresponding to processes in Fig. 1. We also show the non-MEC contribution (R) which is the combined effect of the Darwin-Foldy and spin-orbit terms. These results are calculated with the wave function found from the SdT potential and the three-body force and with the Blatnik-Zovko model for nucleons.

imental electron scattering data at low q ; the IJL and Blatnik-Zovko models incorporate theoretical ideas like vector-meson dominance and depend on a small number of parameters determined again from available electron-nucleon data. We note that the theoretical results for F_C and F_M evaluated with different models begin to deviate from each other at

about 4.5 fm^{-1} and the differences among the four models become extreme in the high- q region above 7.0 fm^{-1} . It is to be noted also that bulk characteristics like a second minimum and a third maximum are present in all cases; the locality of these features, however, and the magnitude of the form factors at the third maximum are dramatically dif-

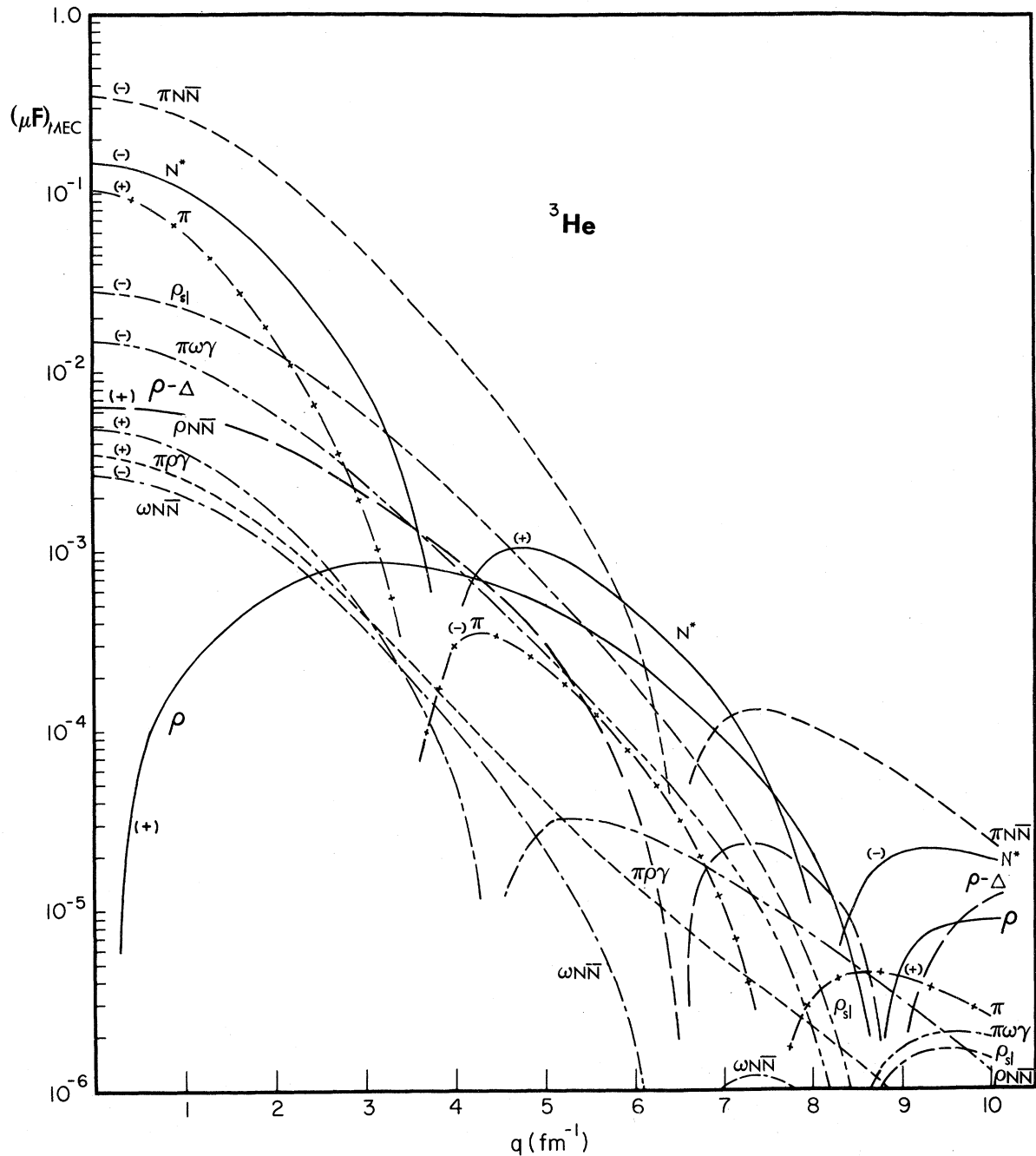


FIG. 9. MEC contributions to the magnetic form factor of ${}^3\text{He}$. For details see Fig. 8.

ferent from model to model. This model dependence is present in both the IA and the MEC contributions to the form factors. As an example we show in Fig. 14 the nucleon model dependence of the MEC contribution to F_C of ${}^3\text{He}$. We emphasize again that it is this substantive model dependence of MEC contributions that makes it impossible to derive unambiguously a (quasi)experimental single-nucleon charge form factor via the subtraction

$F^{\text{exp}} - F(\text{MEC})$ suggested in Ref. 30. It is, in turn, impossible to determine unambiguously the central form of a (quasi)experimental single-nucleon charge density, as discussed in Ref. 29.

Finally, Figs. 12–14 also show the form factor results obtained with point nucleons. The effect of smearing the charge within a finite nucleonic volume is positively dramatic.

We continue now with results showing the sensi-

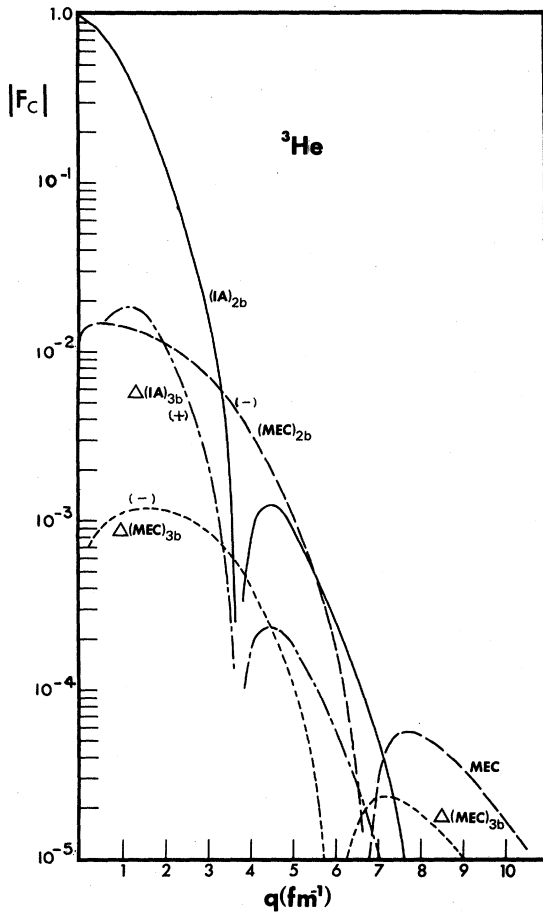


FIG. 10. The IA and MEC results for F_C of ${}^3\text{He}$ evaluated with the SdT potential (no three-body force) and corrections $\Delta(\text{IA})_{3b}, \Delta(\text{MEC})_{3b}$ due to the three-body force.

tivity of the form factors to NN interaction models. Only soft-core NN models have been employed in this work,¹³⁻¹⁶ like the Paris model (P), the Reid model (RSC) and the Sprung-de Turreil super soft core model (SdT). In addition, we have results with the unphysical Malfliet-Tjon potential (MT) for the reason that this model has no tensor component; hence, by comparison with the results evaluated with the realistic models, we may gain an appreciation of the role of the tensor interaction.

One is reminded that the RSC model is fully phenomenological, constructed by fitting NN phase parameters and low-energy data. Neither its short range form nor the central-to-tensor ratio in the important S and D partial waves is unambiguously fixed by the data. The Paris model contains theoretical long and medium range parts arising from one-pion and two-pion exchange and parts of three-pion

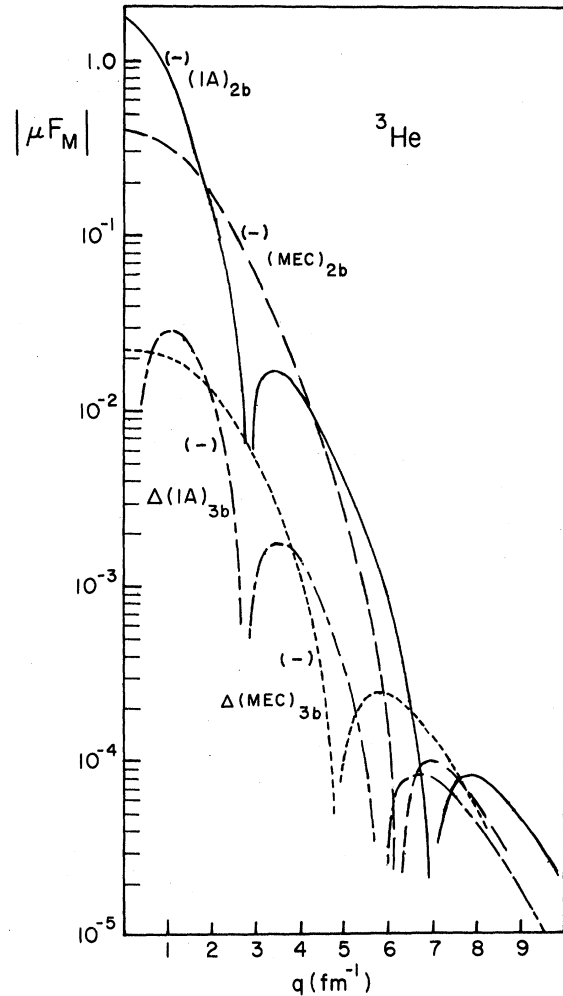


FIG. 11. The IA and MEC results for F_M of ${}^3\text{He}$ evaluated with the SdT potential (no three-body force) and corrections $\Delta(\text{IA})_{3b}, \Delta(\text{MEC})_{3b}$ due to the three-body force.

exchanges (ω and A_1 meson exchanges). The two-pion exchange contributions were derived by means of dispersion relations from pion-nucleon and pion-pion (S and P wave amplitudes) data. The short-range part of the potential is purely phenomenological and velocity-dependent, satisfying the condition that it does not influence the medium- and long-range parts beyond 0.8 fm. The 1977 version of the Paris model is utilized in this work. The SdT model contains theoretical π -, ρ -, and ω -exchange contributions, while additional mesonic exchange effects are taken into account phenomenologically by means of one-boson exchange potential (OBEP) functions with free ranges and amplitudes. Inside 1 fm a phenomenological core is adopted which does not influence the medium- and long-range parts of the potential.

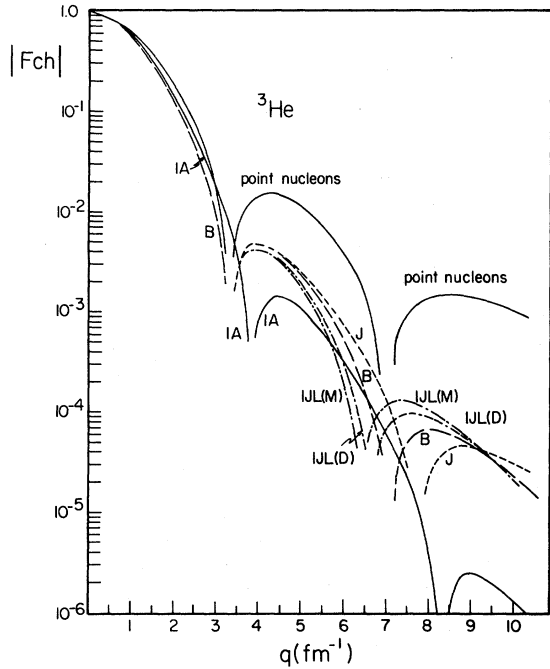


FIG. 12. The dependence of F_C of ${}^3\text{He}$ on nucleon electromagnetic form factor models. These results are evaluated with the SdT potential and the three-body force.

This input translates into a softer repulsion at $r \approx 0.0$ fm and a weaker attraction at intermediate range for the SdT model compared to the Paris

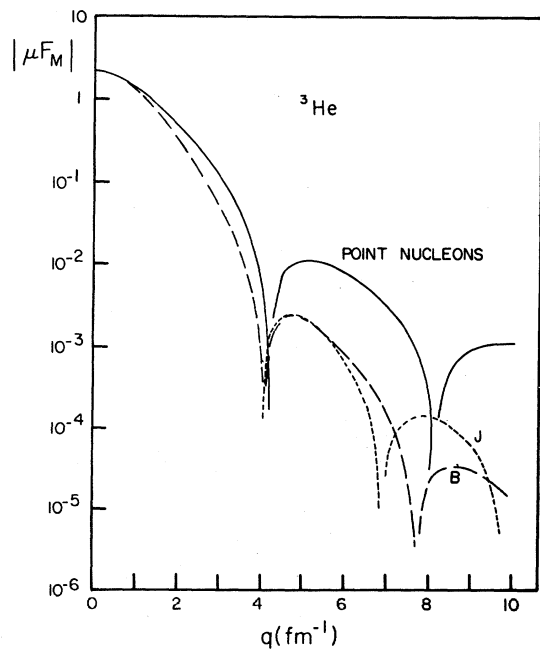


FIG. 13. The dependence of F_M of ${}^3\text{He}$ on nucleon electromagnetic models. These results are evaluated with the SdT potential and the three-body force.

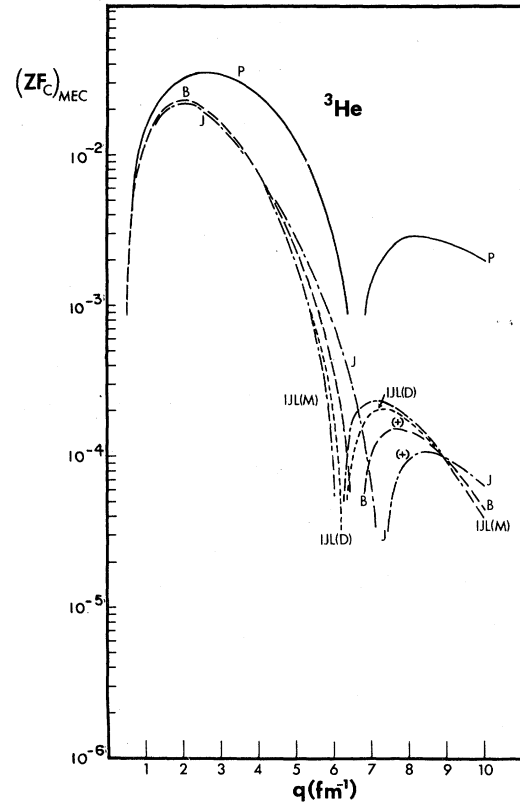


FIG. 14. Nucleon model dependence of MEC contributions to F_C of ${}^3\text{He}$.

model, and for the latter compared to RSC. The value of the triplet effective range is highest for SdT and lowest for RSC. We recall that there are no two-pion or three-pion exchange processes among those in Fig. 1 contributing to the two-body nuclear current employed in the present work. Hence, our sources for MEC appear to be more consistent with the dynamical one-boson exchange (OBE) processes giving rise to the SdT potential model. It may be worthwhile, however, to examine in the future two-pion exchange processes suggested recently in Ref. 31 and shown in Fig. 2(b). These may play a significant role in the region of medium q values.

The dependence of the ${}^3\text{He}$ form factors on NN potential models is shown in Figs. 15 and 16. These results do not include the effect of the three-body force; the Blatnik-Zovko model and $\Lambda_\pi = 6.0$ fm have been utilized here. We note, first of all, the large difference between the predictions from the realistic interaction models and the results obtained with the MT model which has no tensor component. The magnetic form factor reflects more significantly the impact of the tensor interaction because this latter's contribution arises primarily via S -to- D and D -to- S matrix elements of the IA $M1$ operator

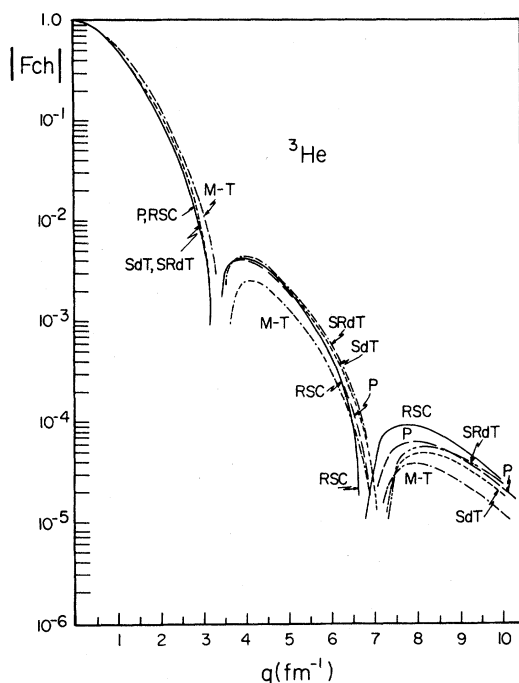


FIG. 15. The dependence of the charge form factor of ${}^3\text{He}$ on NN models. The effects of the three-body force are not included in these results.

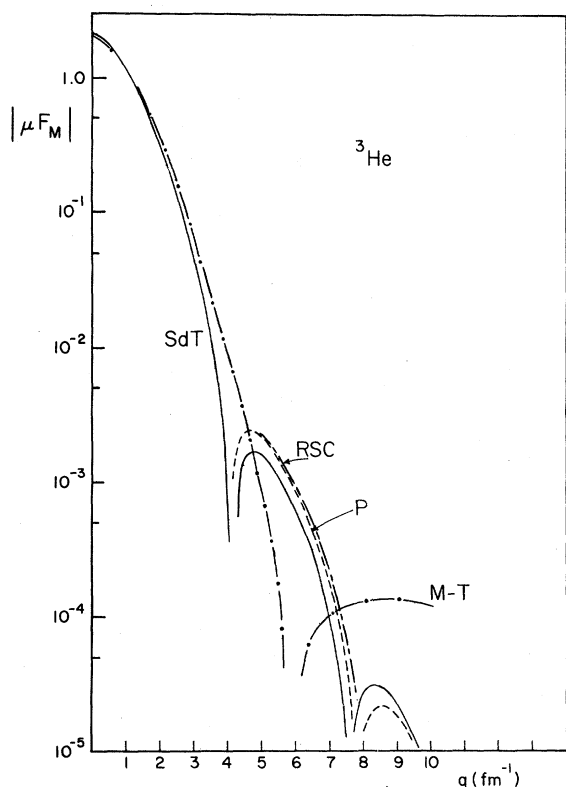


FIG. 16. The dependence of the magnetic form factor of ${}^3\text{He}$ on NN models. The effects of the three-body force have been omitted.

$$T_{1,0}^{\text{MAG}} \sim e/2M \sum_{i=1}^3 \left\{ \frac{1}{2} (F_M^S + \tau_{iz} F_M^V) \sigma_{iz} j_0(qv_i) - \sqrt{2\pi} \frac{1}{2} (F_M^S + \tau_{iz} F_M^V) \otimes [Y_2(\hat{r}_i) \otimes \sigma_i]_0^{(1)} j_2(qr_i) \right\}. \quad (5)$$

This contribution is proportional to the D -state amplitude ($\sim 29\%$), rather than the D -state admixture ($\sim 8\%$) as in the case of the charge form factor where there are nonzero S -to- D matrix elements.

The differences in the short-range behavior among the realistic models begins to be reflected significantly in the three-body form factors only after about $q \sim 7.0 \text{ fm}^{-1}$. Obviously, experimental exploration of this high- q region is strongly suggested by these results also, if we hope to understand the short-range processes in the nuclear medium.

It is worth recalling that tentative attempts to generate NN interactions based on quark dynamics appear to fail to produce a short range repulsion.³² There is, however, considerable uncertainty in the input for these calculations, compounded by the fact that we have no firm convictions as to what to aim for in the short-range regime. The available data do not provide adequate guidelines so far. We may be certain of one point, however, namely, that the short-range NN correlations are very much dependent on the nucleon radius. This dependence can be quantified in simple quark models of the nucleon,³² for example. Very crudely we attempt here to assess the effect of the nucleon size by examining the dependence of the ${}^3\text{He}$ form factors on the meson-nucleon interaction volume as it is reflected in the value of the parameter Λ_π . We limit the discussion to the dominant one pion exchange (OPE) processes and then only as they affect the two-body current.

In Fig. 17 we show the contribution of the πNN process to the charge form factor of ${}^3\text{He}$ as a function of the parameter Λ_π in the monopole π - N form factor, Eq. (3). The values of Λ_π range from 2.0 fm^{-1} corresponding to an interaction volume with a radius of about 0.9 fm to $\Lambda_\pi = 6.0 \text{ fm}^{-1}$ corresponding to a radius of about 0.33 fm . The case with $\Lambda_\pi = \infty$ (point nucleons) is also shown. We note considerable reduction in the MEC effect with nucleon size. A similar trend is observed in Fig. 18 where we present the full magnetic form factor of ${}^3\text{He}$ for four different values of Λ_π , namely, $\Lambda_\pi = \infty$ (point nucleons), 6.0 , 4.0 , and 2 fm^{-1} . A value of $\Lambda_\pi = 5.08 \text{ fm}^{-1}$ was suggested by a recent analysis of $\gamma + p \rightarrow \pi^+ + n$ data.³³ We note again that the MEC result is trivially small for $\Lambda_\pi = 2 \text{ fm}^{-1}$.

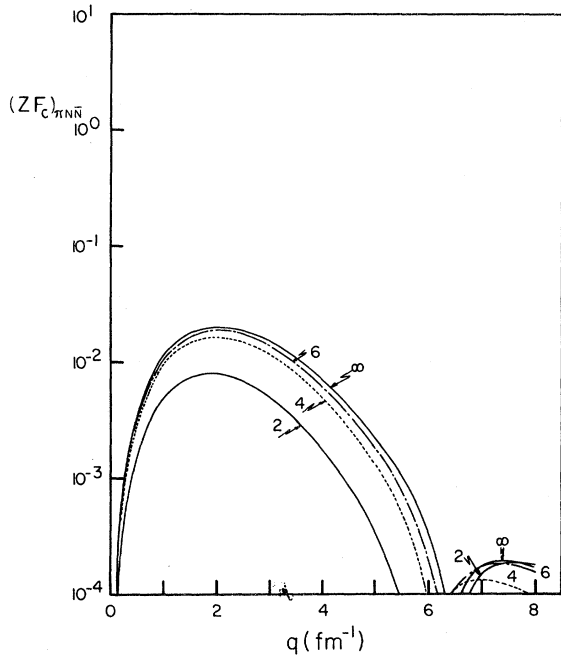


FIG. 17. The contribution of the $\pi N\bar{N}$ process to the charge form factor of ${}^3\text{He}$ as a function of the $\pi N\bar{N}$ vertex parameter Λ_π ($\Lambda_\pi = \infty$ corresponds to point nucleons).

Also, model-dependent calculations of nucleon radii based on chiral quark models of nucleons³⁴ find that the experimental charge rms radius of the proton (0.88 ± 0.03 fm) can be reproduced for a quark

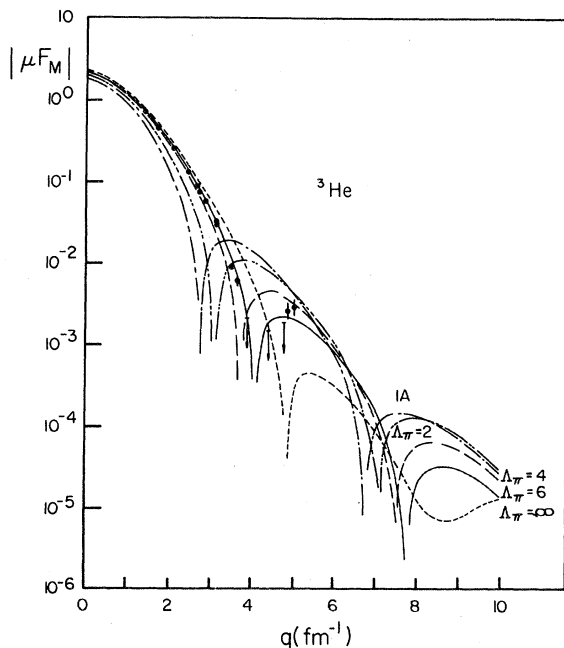


FIG. 18. The magnetic form factor of ${}^3\text{He}$ for four different values of the $\pi N\bar{N}$ vertex parameter Λ_π .

bag radius of about 1.0 fm, while the neutron charge (r^2) radius (-0.12 ± 0.01 fm²) is almost independent of the bag radius. If, indeed, the enhancement of the nuclear current due to the familiar pion-exchange processes in the nuclear medium is drastically reduced, as shown in Figs. 17 and 18, by virtue of nucleons of larger spatial extension than hitherto assumed, then new microscopic processes based on quark degrees of freedom must be found that will furnish the necessary current. Investigations in this area have not yet begun.

In summary, we have explored in this section the dependence of the form factors of ${}^3\text{He}$ on nucleon structure and NN interaction models, and have identified the high q region, $q > 6.0$ fm⁻¹, as the critical region where experimental data of sufficiently good quality can have a strong impact on theoretical ideas regarding short-range processes in the nuclear medium. We find no combination of theoretical models examined in this work which can predict successfully the available ${}^3\text{He}$ data at $q > 6.0$ fm⁻¹ in the case of the charge form factor, and at $q > 5.0$ fm⁻¹ in the case of the magnetic form factor.

IV. DISCUSSION

We have presented results for the charge and magnetic form factors and the corresponding charge and magnetization densities of ${}^3\text{He}$ and ${}^3\text{H}$. We have brought together in these calculations a number of theoretical elements such as two-body currents, isobaric degrees of freedom, a genuine three-body force, considerations of nucleonic size and electromagnetic structure, etc., all within the traditional framework of nuclear physics. Within this framework, we have made no approximations other than to consider nucleons in their static limit and use nucleon electromagnetic form factor models which were constructed on the basis of free nucleon data. In addition, the NN dynamics employed here are of nonrelativistic order (while some of the contributions to the nuclear charge density are of relativistic order). The Coulomb potential is omitted but earlier calculations³⁵ show its effect to be insignificant. We expect that most microscopic processes that contribute nontrivially to the nuclear current have been taken into account in this work. Finally, the three-body force employed here is certainly not complete.³⁶ We find that our theoretical results reproduce the available data in the range of momentum transfer q from zero to about 4.0–6.0 fm⁻¹. Thus we predict correctly charge rms radii and magnetic moments of ${}^3\text{He}$ and ${}^3\text{H}$.

In comparing ${}^3\text{He}$ and ${}^3\text{H}$, we find fairly similar bulk characteristics of the form factors, although the diffraction minima and maxima are slightly

shifted from one nucleus to the other by about 0.5 fm^{-1} . Except for this last feature, our results are in basic agreement, regarding MEC effects to the magnetic form factor, with calculations of Ref. 10.

We speculate that if there are any flaws in the theoretical constructs incorporated in the present calculations, which account for disagreement between our predictions and ${}^3\text{He}$ data at values of q greater than 4.0 to 6.0 fm^{-1} , these flaws will manifest themselves in a qualitatively similar manner in the case of ${}^3\text{H}$ data. Yet, extensive ${}^3\text{H}$ data are now needed because they will supply additional quantitative constraints to our theoretical input.

Assuming that further experimental testing will not change significantly the present ${}^3\text{He}$ data for F_M at $4.0 \text{ fm}^{-1} < q < 6.0 \text{ fm}^{-1}$, and for F_C at $6.0 \text{ fm}^{-1} < q < 8.0 \text{ fm}^{-1}$, we are confronted with serious

discrepancies with theoretical predictions in these q regions. We have shown in Sec. III that these discrepancies cannot be eliminated in the framework of a nonrelativistic theory as long as we rely on NN interaction models and nucleon electromagnetic models based exclusively on traditional meson exchange theories and the elementarity of nucleons. Hence there appears to be a need to augment the theory by considering short-range contributions from quark processes. This is a problem for the immediate future.

ACKNOWLEDGMENT

This work was supported in part by the National Science Foundation and in part by the Natural Sciences and Engineering Council of Canada.

- ¹W. T. Turchinets (private communication); B. Frois (private communication).
- ²E. Hadjimichael, Nucl. Phys. **A312**, 341 (1978).
- ³M. T. Haftel and W. M. Kloet, Phys. Rev. C **15**, 404 (1977); W. M. Kloet and J. A. Tjon, Phys. Lett. **61B** 356 (1976).
- ⁴D. O. Riska and M. Radomski, Phys. Rev. C **16**, 2105 (1977).
- ⁵C. Hajduk *et al.*, Nucl. Phys. **A352**, 413 (1981).
- ⁶A. J. Kallio *et al.*, Nucl. Phys. **A231**, 77 (1974).
- ⁷E. P. Harper, Y. E. Kim, and A. Tubis, Phys. Rev. C **6**, 1601 (1972).
- ⁸E. Hadjimichael, R. Bornais, and B. Goulard, Phys. Rev. Lett. **48**, 583 (1982).
- ⁹A. Barroso and E. Hadjimichael, Nucl. Phys. **A238**, 422 (1975).
- ¹⁰D. O. Riska, Nucl. Phys. **A350**, 227 (1980).
- ¹¹S. L. Adler and Y. Dothan, Phys. Rev. **151**, 1267 (1966); M. Chemtob and M. Rho, Nucl. Phys. **A163**, 1 (1971).
- ¹²J. Torre, J. J. Benayoun, and J. Chauvin, Z. Phys. A **300**, 319 (1981); C. Gignoux and A. Laverne, Nucl. Phys. **A203**, 597 (1973).
- ¹³R. A. Malfliet and J. A. Tjon, Nucl. Phys. **A127**, 161 (1968).
- ¹⁴R. Vinh Mau, Nucl. Phys. **A238**, 381 (1979).
- ¹⁵R. de Tourreil *et al.*, Nucl. Phys. **A242**, 445 (1975); **A273**, 282 (1976).
- ¹⁶R. V. Reid, Ann. Phys. (N.Y.) **50**, 411 (1968).
- ¹⁷R. G. Arnold and F. Gross, MIT report, 1981 (unpublished).
- ¹⁸T. Janssens *et al.*, Phys. Rev. **142**, 1922 (1966).
- ¹⁹F. Iachello, A. D. Jackson, and A. Lande, Phys. Lett. **43B**, 191 (1973).
- ²⁰S. Blatnik and N. Zovko, Acta Phys. Austriaca **39**, 62 (1974).
- ²¹J. S. McCarthy, I. Sick, and R. R. Whitney, Phys. Rev. C **15**, 1396 (1977).
- ²²R. G. Arnold *et al.*, Phys. Rev. Lett. **40**, 1429 (1978).
- ²³H. Collard *et al.*, Phys. Rev. **138**, 357 (1965).
- ²⁴M. Bernheim *et al.*, Lett. Nuovo Cimento **5**, 431 (1972).
- ²⁵P. Dunn, Ph.D. thesis, MIT, 1981 (unpublished); Phys. Rev. C (to be published).
- ²⁶J. M. Cavedon *et al.*, in *Proceedings of the Ninth International Conference on High Energy Physics and Nuclear Structure, Versailles, 1981*, edited by P. Catillon, P. Radvanyi, and M. Porneuf (North-Holland, Amsterdam, 1982).
- ²⁷B. T. Chertok, Phys. Rev. Lett. **41**, 1155 (1978).
- ²⁸M. Namiki, K. Okano, and N. Oshimo, Phys. Rev. C **25**, 2157 (1982).
- ²⁹E. Hadjimichael, R. Bornais, and B. Goulard, Phys. Rev. C **26**, 294 (1982).
- ³⁰I. Sick, in *Lecture Notes in Physics*, **87**, Proceedings of the Eighth International Conference on Few-Body Systems and Nuclear Forces II, Graz, 1978, edited by H. Zingl, M. Haftel, and H. Zankel (Springer, Berlin, 1978), p. 276.
- ³¹A. M. Green and W. Strueve, Phys. Lett. **112B**, 10 (1982).
- ³²See, for example, A. Faessler *et al.*, Phys. Lett. **112B**, 201 (1982), and references therein.
- ³³C. A. Dominguez and R. B. Clark, Phys. Rev. C **21**, 1944 (1980).
- ³⁴F. Myhrer, Phys. Lett. **110B**, 353 (1982).
- ³⁵T. Sasakawa, H. Okemo, and T. Sawada, Phys. Rev. C **23**, 905 (1981).
- ³⁶The subject of the three-body force is still under active investigation. See, for example, R. B. Wiringa, Argonne report (unpublished).